

Direct structure determination of a composite double-layer surface alloy by x-ray photoelectron diffraction: $p(2 \times 2)$ -Na/Al(111)

R. Fasel, P. Aebi, and L. Schlapbach

Institut de Physique, Université de Fribourg, 1700 Fribourg, Switzerland

J. Osterwalder

Physik-Institut, Universität Zürich-Irchel, Winterthurerstrasse 190, 8057 Zürich, Switzerland

The local structure of $p(2 \times 2)$ -Na/Al(111) has been investigated using angle-scanned full hemispherical x-ray photoelectron diffraction. The resulting diffraction patterns allow a *direct* and *unequivocal* determination of the surface atomic structure. Even though Na and Al are completely immiscible in the bulk, the $p(2 \times 2)$ -Na/Al(111) phase consists of a *composite double-layer surface alloy* where Na atoms take substitutional and fcc hollow sites and Al atoms removed from the surface occupy hcp hollow sites.

Quantitative structural information is fundamental to the understanding of surface properties, e.g., for the interpretation of spectroscopic results or as a starting point for theoretical calculations. The most prominent quantitative structural methods, such as low-energy electron diffraction (LEED) or surface extended x-ray absorption fine-structure spectroscopy (SEXAFS), rely to a great extent on a trial-and-error approach in which experimental and theoretical curves are compared. Therefore, structural information is not provided directly, and only structures which are explicitly taken into account in the analysis can be found. This limits the applicability of these methods, especially in the case of complex and unanticipated surface structures. For this reason, much effort has recently been put into the development of direct methods that yield at least approximate structures directly from the data.¹ These then serve as a starting point for a more precise structure search. In previous publications^{2,3} we have shown that full hemispherical x-ray photoelectron diffraction (XPD) patterns in many cases give very direct information about the near surface structure. The application of XPD to complex systems to determine reliable and direct structural information is very promising. In this paper we report on XPD results of the $p(2 \times 2)$ -Na/Al(111) adsorption geometry where the Na KVV and Na $1s$ diffraction patterns allow a *direct* and *unequivocal* determination of the unusual atomic structure of this phase. Furthermore, precise structural parameters have been obtained using an R -factor analysis of single scattering cluster (SSC) calculations.

The adsorption systems of alkali metals on Al would seem superficially to be very simple, involving two nearly-free-electron metal species. In reality, these appear to be far from simple in their behavior.⁴ Traditional expectations are that the alkali atoms adsorb in the most highly coordinated position on a practically undisturbed surface. However, high-resolution core-level photoelectron spectroscopy has shown that the room-temperature (RT) adsorption of Na, K, Rb, and Cs on Al(111), as well as the adsorption of Na on Al(001), leads to a disruption of the Al surface and to the formation of a surface alloy.⁵⁻⁷ For Na/Al(111), the sequence of ordered structures typical for other close-packed surfaces, that is, a

$p(2 \times 2)$ followed by a $(\sqrt{3} \times \sqrt{3})R30^\circ$ structure (hereafter called $\sqrt{3}$ structure), is inverted, and the characteristic "ring phase" at low coverages is absent.⁷ The structure of the $\frac{1}{2}$ ML $\sqrt{3}$ phase has been determined using various methods,⁸⁻¹⁰ and there is general agreement in that it consists of Na atoms adsorbed in substitutional sites where every third Al surface atom is removed.

The structure of the 0.5 ML $p(2 \times 2)$ phase, however, has remained a challenge for many years. Since the early study of Porteus,¹¹ suggesting a three-domain model with a $p(2 \times 1)$ periodicity, different and contradictory models have been proposed.^{5,12-14} Very recently, the first step towards the solution of the $p(2 \times 2)$ -Na/Al(111) puzzle was made by Stampfl and Scheffler.¹⁵ On the basis of density-functional-theory (DFT) calculations, these authors have shown that the adsorption energies for the structures proposed thus far are clearly less favorable than those of a structure involving two intermixed Na-Al layers, where Na atoms take substitutional and fcc hollow sites and Al atoms occupy hcp hollow sites. This unusual structure has been rationalized with the argument that both species of atoms in the composite double layer may experience an optimum charge density, because each is in a highly coordinated position with Al-Al and Na-Na bond lengths similar to their bulk values. Following this, a combined SEXAFS and LEED study¹⁶ of the $p(2 \times 2)$ -Na/Al(111) structure was performed. The SEXAFS data are compatible with the model proposed by Stampfl and Scheffler,¹⁵ but do not argue or reject against alternative models. From the three structural models taken into account in the LEED analysis, the double-layer model of Stampfl and Scheffler is clearly favored.

However, a direct confirmation of the aforementioned structural model is clearly desirable. Full hemispherical XPD patterns provide very direct information about the near-surface structure. At electron kinetic energies above 500 eV, the strongly anisotropic scattering of the electrons by the ion cores leads to a forward focusing of electron flux along the emitter-scatterer axis. Prominent intensity maxima can therefore often be identified with bond directions. One finds that the photoelectron angular distribution is, to a first approxi-

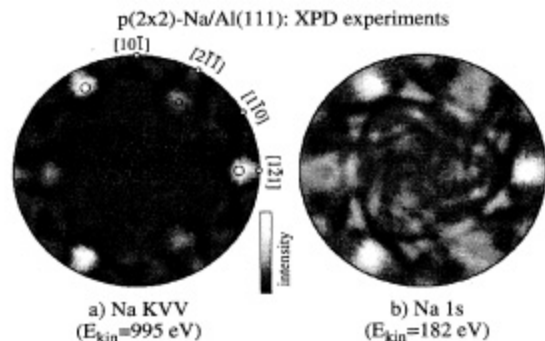


FIG. 1. Experimental XPD patterns from $p(2 \times 2)$ -Na/Al(111): (a) Na KVV at 995 eV kinetic energy, and (b) Na $1s$ at 182 eV kinetic energy. The data have been stereographically projected and normalized according to the procedure described in the text. Forward-focusing directions are indicated in the Na KVV pattern.

mation, a forward-projected image of the atomic structure around the photoemitter. Analysis of the symmetry and positions of forward-focusing maxima permit a very straightforward structural interpretation of XPD data.²

Experiments were performed in a VG ESCALAB Mark II spectrometer modified for motorized sequential angle-scanning data acquisition, and with a base pressure in the lower 10^{-11} -mbar region. Photoelectron spectra and diffraction patterns were measured using Mg $K\alpha$ ($h\nu = 1253.6$ eV) radiation. The samples were maintained at about 250 K during the measurements. Contamination-free surfaces were prepared by a combination of Ar^+ sputtering and annealing at 500 °C. Na was evaporated from carefully outgassed SAES getter sources while the crystal was maintained at RT. During Na deposition the pressure was in the lower 10^{-10} -mbar range. The purity of the deposited Na layers, as well as the coverage, was checked by core-level photoemission. The LEED pattern of the Na overlayers showed overlayer spots almost as sharp as the substrate spots, and a low background, indicating a high degree of long-range order.

Experimental diffraction patterns of the Na KVV peak at 995 eV and the Na $1s$ peak at 182 eV kinetic energy are shown in Figs. 1(a) and 1(b). The patterns have been azimuthally averaged exploiting the threefold rotational symmetry of the system, and normalized with respect to the mean intensity for each polar emission angle. The patterns are shown in stereographic projection. The center of each plot corresponds to the surface normal and the outer circle represents grazing emission along the surface. From the high-energy Na KVV diffraction pattern, which represents a forward-projected image of the atomic structure above the Na emitters, it is immediately evident that more than one layer must be involved in the formation of the $p(2 \times 2)$ structure. The appearance of six forward-focusing peaks at nongrazing emission angles in the Na KVV diffraction pattern excludes all two-dimensional models. In particular, it excludes the model proposed in Ref. 11 consisting of three domains each with $p(2 \times 1)$ periodicity. The absence of forward-focusing peaks at small emission angles excludes all models containing atoms on top of Na atoms. The model involving two reconstructed layers of stoichiometry $NaAl_2$ proposed in Ref. 13 can thus also be ruled out, as well as the

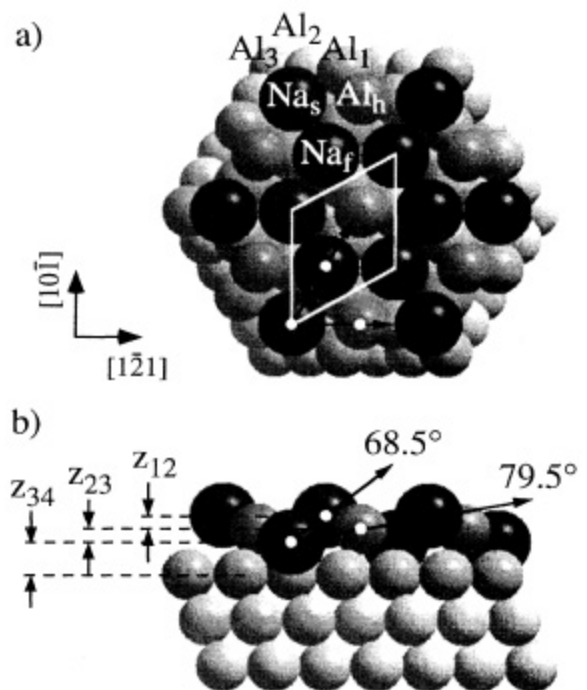


FIG. 2. (a) Top and (b) front views of the proposed surface structure of $p(2 \times 2)$ -Na (black) on Al(111). The interatomic directions accounting for the forward-focusing peaks [indicated in Fig. 1(a)] are marked by arrows. The atoms are labeled with a subscript indicating the corresponding adsorption site: f (fcc hollow site), h (hcp hollow site), s (substitutional site), 1–3 (first–third substrate layer).

double-layer model of distorted bcc Na(111) planes,¹² which cannot account for the two inequivalent forward-focusing directions seen in the Na KVV diffraction pattern.

The Na coverage of the $p(2 \times 2)$ structure is 0.5 ML, and the unit cell therefore contains two Na atoms. Considering this fact, the structure of the $p(2 \times 2)$ -Na/Al(111) phase can be unequivocally determined from the positions of the forward-focusing peaks in the Na KVV diffraction pattern. These forward-focusing peaks emerge at polar emission angles of 79.5° in the angle $\langle 1\bar{2}1 \rangle$ azimuths and 68.5° in the $\langle 2\bar{1}\bar{1} \rangle$ azimuths. As there are only two Na atoms per $p(2 \times 2)$ unit cell, these two different forward-focusing directions cannot be explained by Na scattering only; an additional Al atom must be involved. The only possible way to arrange these three atoms in the $p(2 \times 2)$ unit cell, respecting the observed forward-focusing directions and physically meaningful bond lengths, is shown in Fig. 2. The $p(2 \times 2)$ unit cell is formed as follows: a Na atom is substituted for a surface Al atom (Na_s), an Al atom is adsorbed in the hcp hollow site (Al_h), and an additional Na atom is adsorbed in the fcc hollow site (Na_f). The inverse situation (Na_s , Na_h , Al_f), with the Al atom adsorbed in the fcc site and the Na atom adsorbed in the hcp site, can be excluded because it would give rise to a forward-focusing peak at about 67° in the $\langle 1\bar{2}1 \rangle$ azimuth, which is not observed. The first two in-

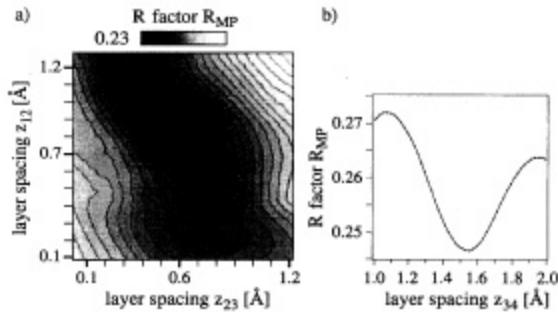


FIG. 3. (a) R -factor contour plot obtained by varying the first two interlayer spacings z_{12} and z_{23} for the SSC calculations. The combined data set (Na KVV and Na $1s$ diffraction patterns) has been used for the calculation of this R factor. (b) R -factor curve obtained by varying the layer spacing z_{34} for the Na $1s$ SSC calculations.

terlayer spacings z_{12} and z_{23} , as determined from the observed polar emission angles, are 0.7 and 0.6 Å, respectively. In Fig. 2, the interatomic directions corresponding to the forward-focusing peaks in the Na KVV diffraction pattern of Fig. 1(a) are indicated by arrows. A comparison of the structural model (Fig. 2) and the Na KVV diffraction pattern of this structure [Fig. 1(a)] demonstrates well that the atomic arrangement of this double-layer surface alloy is directly reflected in the diffraction pattern.

The structural model discussed above and shown in Fig. 2 is, in fact, identical to the DFT-based model proposed by Stampfl and Scheffler.¹⁵ To determine the structural parameters to a higher degree of precision we have performed SSC calculations and an R -factor analysis for both the Na $1s$ and the Na KVV diffraction patterns. Diffraction patterns were calculated using a SSC code as implemented by Friedman and Fadley,¹⁷ which includes spherical wave corrections.¹⁸ The proper s initial state has been taken into account for the low-energy Na $1s$ pattern, and s -wave emission has been used to model the high-energy Na KVV Auger emission.¹⁹ To judge the quality of the fit between calculation and experiment a new R -factor (R_{MP}) has been used. This R -factor is based on the space of multipole coefficients rather than emission angles.²⁰ A systematic multiparameter search was performed. The structural parameters, as well as the “effective” inner potential V_0 (responsible for the refraction at the surface-potential barrier),²⁰ and the electron inelastic mean free path Λ_e were all varied in the calculations.

The R -factor plot obtained by varying the first two interlayer spacings z_{12} and z_{23} around the geometrical values of 0.7 and 0.6 Å is shown in Fig. 3(a).²¹ It can be seen from this contour plot that the “true” structural parameters yielding the best fit are not far from the initial values determined by purely geometrical considerations. The minima of the individual R -factor plots for the Na KVV and Na $1s$ diffraction patterns (not shown) are found at identical locations in parameter space, which provides further confidence in the reliability of the results. In a further step we have also included a variation of the third-to-fourth layer spacing z_{34} in the analysis of the Na $1s$ diffraction pattern. It is expected that the low-energy Na $1s$ diffraction pattern is more sensi-

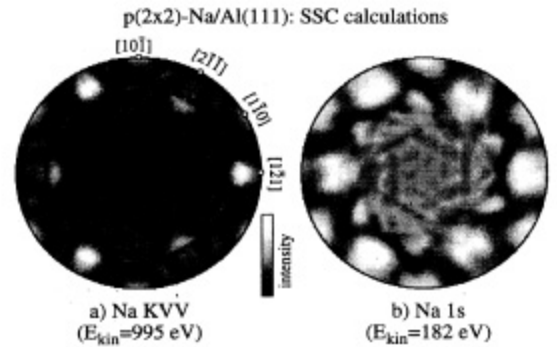


FIG. 4. SSC calculations for the best-fit geometry depicted in Fig. 2: (a) Na KVV at 995 eV kinetic energy, and (b) Na $1s$ at 182 eV kinetic energy.

tive to the position of this layer below the Na emitters. The dependence of the R factor on layer spacing z_{34} is shown in Fig. 3(b). After overall optimization we obtain layer spacings of $z_{12}=0.85$ Å, $z_{23}=0.55$ Å, and $z_{34}=1.54$ Å, where the indices denote the layers starting from the uppermost Na layer. The SSC calculations for this best-fit geometry are shown in Fig. 4. Remarkable agreement with experimental results (Fig. 1) is obtained even in fine structural features.

In Table I we give a comparison of the interlayer spacings determined in this work with the corresponding values from Ref. 16. It can be seen that the first three interlayer spacings determined by XPD and by LEED agree to within 0.02 Å, whereas the values determined by SEXAFS and by DFT deviate slightly more from the XPD/LEED values. Nevertheless, given the complexity of the $p(2 \times 2)$ -Na/Al(111) structure, the level of agreement between the results derived from different methods is very satisfactory.

The formation of the $p(2 \times 2)$ double-layer structure is of great interest. At first glance, this formation appears to involve no mass transport over large distances, because the number of surface vacancies created by the first Na layer equals the number of Al atoms adsorbed in the hcp hollow sites. However, the $p(2 \times 2)$ structure starts growing only after completion of the $\sqrt{3}$ structure, which consists of $\frac{1}{3}$ ML Na atoms adsorbed in the substitutional sites. The Al atoms removed from the surface during the formation of this phase are not incorporated into the $\sqrt{3}$ structure. It has been argued

TABLE I. Interlayer spacings z_{ij} (Å) determined in this work compared with the corresponding values obtained from Ref. 16. The layers are numbered from the surface into the bulk. The atomic species of each layer is given with a subscript indicating the corresponding adsorption site: f (fcc hollow site), h (hcp hollow site), s (substitutional site), 1 (first substrate layer).

Layer	1	2	3	4
Atom species	Na _{<i>f</i>}	Al _{<i>h</i>}	Na _{<i>s</i>}	Al ₁
Interlayer spacing	z_{12}	z_{23}	z_{34}	
XPD (this work)	0.85	0.55	1.54	
LEED (Ref. 16)	0.85	0.55	1.52	
SEXAFS (Ref. 16)	0.75	0.70	1.50	
DFT (Ref. 16)	0.72	0.62	1.46	

that they diffuse to surface steps where they can be readsorbed.⁸ The formation of the $p(2 \times 2)$ phase thus involves a large mass transport, as $\frac{1}{3}$ ML additional Al atoms must be reincorporated. During the formation of this phase it has been observed by scanning tunneling microscopy¹⁴ that holes are formed on large terraces. At least a portion of the Al atoms reincorporated in the $p(2 \times 2)$ structure are therefore *displaced from the surface*. Steps might act as additional sources of substrate atoms.

In conclusion, we have performed full hemispherical XPD measurements of the $p(2 \times 2)$ -Na/Al(111) phase. The atomic arrangement of this structure could be determined *unequivocally* from experimental results using simple geometrical considerations. Our findings agree with a recent combined

DFT, LEED, and SEXAFS study. We conclude that the unit cell of this composite double-layer surface alloy structure consists of one Na atom substituting a surface Al atom, an additional Na atom in the fcc adsorption site, and an Al atom in the hcp adsorption site. By means of an R -factor analysis, which compares the experimental diffraction patterns to SSC calculations, detailed structural parameters have been determined.

We thank R. G. Agostino for many invaluable discussions. Skillful technical assistance was provided by E. Mooser, O. Raetz, F. Bourqui, and H. Tschopp. This project has been supported by the Fonds National Suisse pour la Recherche Scientifique.

- ¹J. J. Barton, Phys. Rev. Lett. **61**, 1356 (1988); D. K. Saldin and P. L. de Andres, *ibid.* **64**, 1270 (1990); for a review, see also J. Osterwalder, R. Fasel, A. Stuck, P. Aebi, and L. Schlapbach, J. Electron Spectrosc. Relat. Phenom. **68**, 1 (1994).
- ²J. Osterwalder, P. Aebi, R. Fasel, D. Naumovic, P. Schwaller, T. Kreutz, L. Schlapbach, T. Abukawa, and S. Kono, Surf. Sci. (to be published).
- ³R. Fasel, P. Aebi, J. Osterwalder, and L. Schlapbach, Surf. Sci. (to be published).
- ⁴R. Fasel and J. Osterwalder, Surf. Rev. Lett. (to be published); C. Stampfl and M. Scheffler, *ibid.* (to be published); J. N. Andersen, *ibid.* (to be published).
- ⁵J. N. Andersen, M. Qvarford, R. Nyholm, J. F. van Acker, and E. Lundgren, Phys. Rev. Lett. **68**, 94 (1991).
- ⁶J. N. Andersen, E. Lundgren, R. Nyholm, and M. Qvarford, Phys. Rev. B **46**, 12 784 (1992).
- ⁷J. N. Andersen, E. Lundgren, R. Nyholm, and M. Qvarford, Surf. Sci. **289**, 307 (1993).
- ⁸A. Schmalz, S. Aminpirooz, L. Becker, J. Haase, J. Neugebauer, M. Scheffler, D. R. Batchelor, D. L. Adams, and E. Bøgh, Phys. Rev. Lett. **67**, 2163 (1991).
- ⁹M. Kerker, D. Fisher, D. P. Woodruff, R. G. Jones, R. D. Diehl, and B. Cowie, Phys. Rev. Lett. **68**, 3204 (1992).
- ¹⁰J. Burchhardt, M. M. Nielsen, D. L. Adams, E. Lundgren, and J. N. Andersen, Phys. Rev. B **50**, 4718 (1994).
- ¹¹J. O. Porteus, Surf. Sci. **41**, 515 (1974).
- ¹²A. Hohlfeld and K. Horn, Surf. Sci. **211/212**, 844 (1989).
- ¹³M. Kerker, D. Fisher, D. P. Woodruff, R. G. Jones, R. D. Diehl, and B. Cowie, Surf. Sci. **278**, 246 (1992).
- ¹⁴H. Brune, J. Winterlin, R. J. Behm, and G. Ertl, Phys. Rev. B **51**, 13 592 (1995).
- ¹⁵C. Stampfl and M. Scheffler, Surf. Sci. **319**, L23 (1994).
- ¹⁶J. Burchhardt, M. M. Nielsen, D. L. Adams, E. Lundgren, J. N. Andersen, C. Stampfl, M. Scheffler, A. Schmalz, S. Aminpirooz, and J. Haase, Phys. Rev. Lett. **74**, 1617 (1995).
- ¹⁷D. J. Friedman and C. S. Fadley, J. Electron Spectrosc. Relat. Phenom. **51**, 689 (1990).
- ¹⁸J. J. Rehr, R. C. Albers, C. R. Natoli, and E. A. Stern, Phys. Rev. B **34**, 4350 (1986).
- ¹⁹Even if this is a conceptual oversimplification for the complicated final state arising in Auger emission, it has proven adequate at higher kinetic energies above about 500 eV. See, e.g., S. A. Chambers, Surf. Sci. Rep. **16**, 261 (1992).
- ²⁰R. Fasel, P. Aebi, J. Osterwalder, L. Schlapbach, R. G. Agostino, and G. Chiarello, Phys. Rev. B **50**, 14 516 (1994).
- ²¹In all the calculations shown here, the optimum values of 7.5 eV for V_0 and of 4 and 10 Å for Λ_c (Na 1s and Na KVV, respectively) have been used.

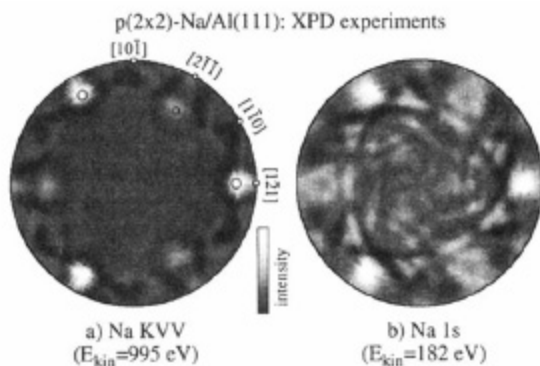


FIG. 1. Experimental XPD patterns from $p(2\times 2)$ -Na/Al(111): (a) Na *KVV* at 995 eV kinetic energy, and (b) Na *1s* at 182 eV kinetic energy. The data have been stereographically projected and normalized according to the procedure described in the text. Forward-focusing directions are indicated in the Na *KVV* pattern.

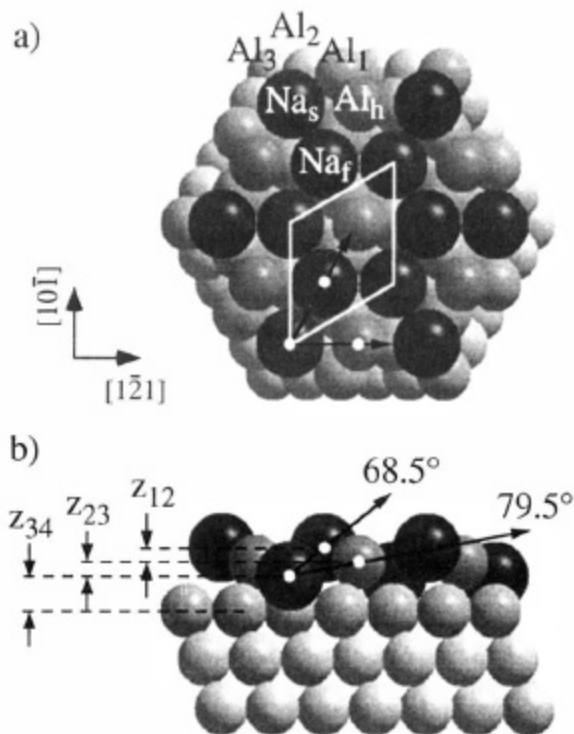


FIG. 2. (a) Top and (b) front views of the proposed surface structure of $p(2\times 2)$ -Na (black) on Al(111). The interatomic directions accounting for the forward-focusing peaks [indicated in Fig. 1(a)] are marked by arrows. The atoms are labeled with a subscript indicating the corresponding adsorption site: *f* (fcc hollow site), *h* (hcp hollow site), *s* (substitutional site), 1–3 (first–third substrate layer).

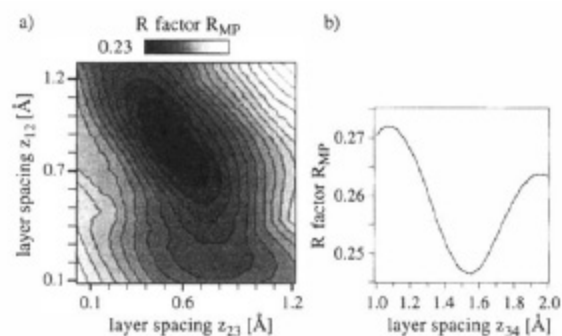


FIG. 3. (a) R -factor contour plot obtained by varying the first two interlayer spacings z_{12} and z_{23} for the SSC calculations. The combined data set (Na KVV and Na $1s$ diffraction patterns) has been used for the calculation of this R factor. (b) R -factor curve obtained by varying the layer spacing z_{34} for the Na $1s$ SSC calculations.

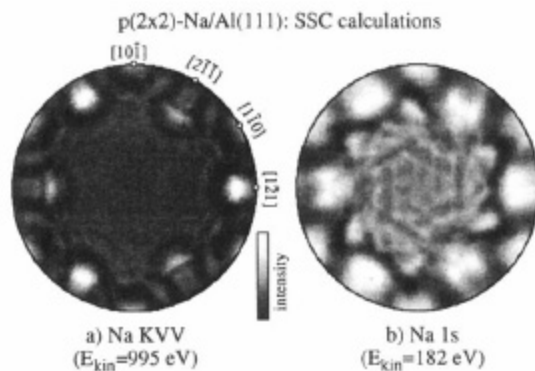


FIG. 4. SSC calculations for the best-fit geometry depicted in Fig. 2: (a) Na KVV at 995 eV kinetic energy, and (b) Na $1s$ at 182 eV kinetic energy.